

Fracture of Brittle Thin Films on Compliant Substrates

Haixia Mei and Rui Huang

Department of Aerospace Engineering and Engineering Mechanics, University of Texas at Austin, Austin, Texas 78712, USA

Abstract

Two different fracture mechanisms of brittle thin films on compliant substrates have been observed, one with interfacial delamination and the other with substrate penetration. Using a set of finite element models, we analyze the effects of delamination and penetration on channel cracking of brittle thin films. The competition between delamination and penetration is examined with respect to the toughness ratio between the substrate and the interface as well as the elastic mismatch. A cohesive zone model is developed to simulate initiation and growth of delamination or penetration cracks from the root of a channel crack.

1. Introduction

Integrated structures with mechanically soft components have recently been pursued over a wide range of novel applications, from high performance integrated circuits in microelectronics [1-3] to unconventional organic and stretchable electronics [4-5]. Channeling cracks in brittle thin films have been observed to be a key reliability issue [2, 3]. Previous studies have shown that the driving force (i.e., the energy release rate) for the steady-state growth of a channel crack in an elastic film depends on the constraint effect of surrounding layers [6]. For a brittle thin film on an elastic substrate, the driving force increases for increasingly compliant substrates [7,8]. The effect of constraint can be partly lost as the substrate deforms plastically [9] or viscoelastically [10, 11]. More recent studies have focused on the effects of stacked buffer layers [3, 12] and patterned film structures [2]. In most of these studies, the interfaces between the film and the substrate or the buffer layers are assumed to remain perfectly bonded as the channel crack grows in the film (Fig. 1a). However, the stress concentration at the root of the channel crack may lead to interfacial delamination (Fig. 1b) or penetration into substrates (Fig. 1c). He and Hutchinson [13] examined the competition between crack deflection into the interface and penetration into the substrate, based on asymptotic solutions for the respective energy release rates. Ye et al. [14] showed that the driving force for channel cracking depends on the channel cross section governed by the fracture properties of the interface and the substrate. More recently, Mei et al. [15] showed that depending on the elastic mismatch and interface toughness, a channel crack may grow with no delamination, with a stable delamination, or with unstable delamination. An effective energy release rate for the steady-state growth of a channel crack was defined to account for the influence of interfacial delamination on both the fracture driving force and the resistance. The roles of toughness and cohesive strength on crack deflection at interfaces were analyzed by Parmigiani and Thouless [16] using a cohesive-zone model.

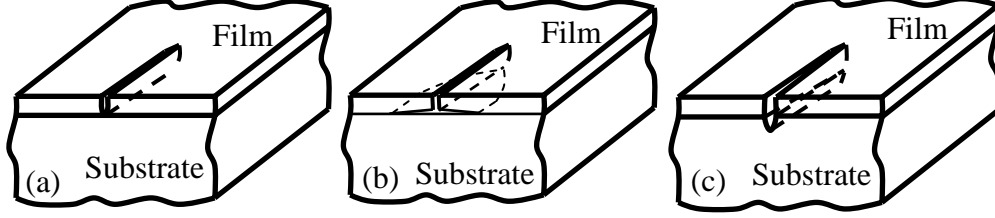


Fig. 1: Schematic illustrations of (a) channel cracking, (b) concomitant channel cracking and interfacial delamination, and (c) concomitant channel cracking and substrate penetration.

In this paper we analyze the effects of interfacial delamination and substrate penetration on channel cracking of brittle thin films, with an emphasis on the cases with elastically compliant substrates. The competition between delamination and penetration is first examined based on a linear elastic fracture mechanics (LEFM) approach and then investigated by a cohesive zone model.

2. Channel Cracking

As illustrated in Fig. 1a, assuming no interfacial delamination, the energy release rate for steady-state growth of a channel crack in an elastic film bonded to a thick elastic substrate is [6-8]:

$$G_{ss} = Z(\alpha, \beta) \frac{\sigma_f^2 h_f}{\bar{E}_f}, \quad (1)$$

where σ_f is the tensile stress in the film, h_f is the film thickness, and $\bar{E}_f = E_f / (1 - \nu_f^2)$ is the plane-strain modulus of the film with Young's modulus E_f and Poisson's ratio ν_f . The dimensionless coefficient Z depends on the elastic mismatch between the film and the substrate, through two Dundurs' parameters

$$\alpha = \frac{\bar{E}_f - \bar{E}_s}{\bar{E}_f + \bar{E}_s}, \quad \beta = \frac{\bar{E}_f(1 - \nu_f)(1 - 2\nu_s) - \bar{E}_s(1 - \nu_s)(1 - 2\nu_f)}{2(1 - \nu_f)(1 - \nu_s)(\bar{E}_f + \bar{E}_s)}. \quad (2)$$

When the film and the substrate have identical elastic moduli, we have $\alpha = \beta = 0$ and $Z = 1.976$. The value of Z decreases slightly for a compliant film on a relatively stiff substrate ($\alpha < 0$), but increases rapidly for compliant substrates ($\alpha > 0$), with $Z > 30$ for $\alpha > 0.99$. Throughout this paper we take $\beta = \alpha/4$.

3. Interfacial Delamination

Consider an interface crack emanating from the channel root at each side (Fig. 1b). For a long, straight channel crack, we assume a steady state far behind the channel front, where the interfacial crack has a finite width, d . The energy release rate for the interfacial crack can be written as

$$G_d = Z_d \left(\frac{d}{h_f}, \alpha, \beta \right) \frac{\sigma_f^2 h_f}{\bar{E}_f}, \quad (3)$$

where Z_d is a dimensionless function that can be determined from a two-dimensional finite element model [15]. As shown in Fig. 2, the Z_d function has two limits. When $d/h_f \rightarrow \infty$ (long crack limit), the interfacial crack reaches a steady state with the energy release rate

$$G_d^{ss} = \frac{\sigma_f^2 h_f}{2E_f}, \quad (4)$$

and thus $Z_d \rightarrow 0.5$. The steady-state energy release rate for the interfacial crack is independent of the elastic mismatch. On the other hand, when $d/h_f \rightarrow 0$ (short crack limit), the interfacial energy release rate follows a power law [13]:

$$Z_d \sim \left(\frac{d}{h_f} \right)^{1-2\lambda}, \quad (5)$$

where λ depends on the elastic mismatch and can be determined by solving the equation

$$\cos \lambda \pi = \frac{2(\alpha - \beta)}{1 - \beta} (1 - \lambda)^2 - \frac{\alpha - \beta^2}{1 - \beta^2}. \quad (6)$$

Three scenarios at the short crack limit can be observed from Fig. 2 and Eq. (5). First, when $\alpha = \beta = 0$ (no elastic mismatch), we have $\lambda = 0.5$. In this case, Z_d approaches a constant as $d/h_f \rightarrow 0$. An analytical solution [17] predicts that $Z_d(0,0,0) = 0.9878$, which compares closely with the numerical results in Fig. 2. When $\alpha > 0$, we have $\lambda > 0.5$. Consequently, $Z_d \rightarrow \infty$ as $d/h_f \rightarrow 0$. For both $\alpha = 0$ and $\alpha > 0$, the energy release rate monotonically decreases as the delamination width increases. On the other hand, when $\alpha < 0$, we have $0 < \lambda < 0.5$, and thus, $Z_d \rightarrow 0$ as $d/h_f \rightarrow 0$.

A necessary condition for steady-state channel cracking with concomitant interfacial delamination is that the interfacial crack arrests at a finite width. The delamination width can be determined by comparing the interfacial energy release rate in Eq. (3) to the interface toughness. In general, the interface toughness depends on the phase angle of mode mix [6], which in turn depends on the delamination width. It was found that the phase angle quickly approaches a steady state value, $\psi_{ss} = \omega(\alpha, \beta)$, which was given in [18]. When $\alpha = \beta = 0$, we have

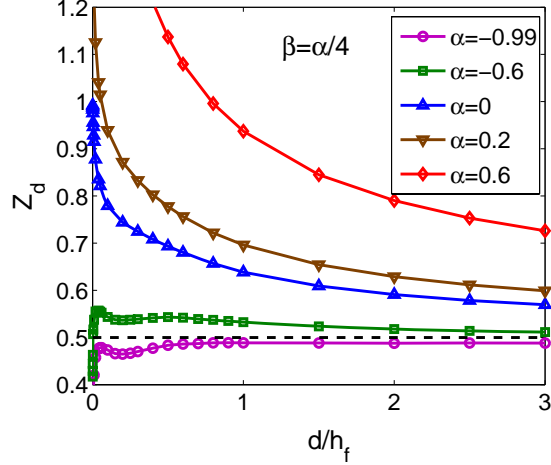


Fig. 2: Normalized energy release rate of interfacial delamination from the root of a channel crack as a function of the normalized delamination width for different elastic mismatch parameters.

$\psi_{ss} = \omega(0,0) = 52^\circ$. Considering the fact that the variation of the phase angle is relatively small and confined within a small range of short cracks ($d < h_f$), we take the phase angle as a constant in the subsequent discussions and assume that the interface toughness is independent of the delamination width, i.e., $\Gamma_i = \Gamma_i(\psi_{ss})$. Then, the width of interfacial delamination can be determined by setting

$$Z_d\left(\frac{d_s}{h_f}, \alpha, \beta\right) = \bar{\Gamma}_i = \frac{\Gamma_i}{\Sigma}. \quad (7)$$

where $\Sigma = \sigma_f^2 h_f / \bar{E}_f$. Depending on the elastic mismatch parameters and the normalized interface toughness ($\bar{\Gamma}_i$), Eq. (7) predicts no delamination, stable finite delamination, or unstable delamination, which is summarized in Fig. 3 as an interfacial delamination map [15]. In particular, for a stiff film on a relatively compliant substrate ($\alpha > 0$), a stable delamination along the channel crack is predicted when $\bar{\Gamma}_i > 0.5$, whereas unstable delamination is predicted when $\bar{\Gamma}_i \leq 0.5$. On the other hand, on a

relatively stiff substrate ($\alpha < 0$), the film cracks with no delamination in Region I. The boundary between Region I and Region II-B is determined from the finite element calculations, corresponding to the maximum interfacial energy release rate in the range $0 > \alpha > -0.89$. In an experimental study by Tsui et al. [3], no interfacial delamination was observed for channel cracking of a low k film directly deposited on a Si substrate, while a finite delamination was observed when a compliant buffer layer was sandwiched between the low k film and the substrate. These observations are consistent with the delamination map.

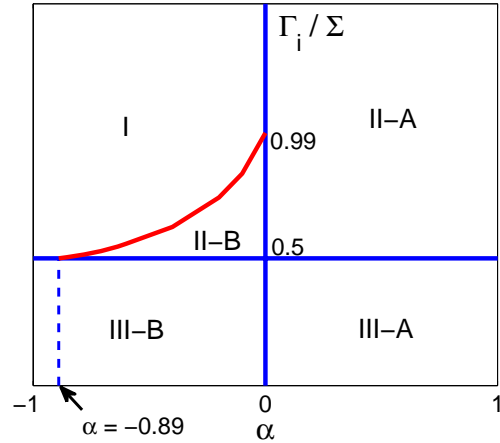


Fig. 3. A map for interfacial delamination from the root of a channel crack: (I) no delamination, (II) stable delamination, and (III) unstable delamination, where A and B denote delamination without and with an initiation barrier, respectively.

4. Channel Cracking with Delamination

In this section, we study the fracture mode that channel cracking in an elastic thin film on a relatively compliant substrate is accompanied by interfacial delamination, either stable or unstable, depending on the interface toughness. This differs from the case for an elastic film on a relatively stiff substrate, where channel cracks may grow without interfacial delamination (Region I in Fig. 3).

With a stable delamination along each side of the channel crack (Fig. 1b), the substrate constraint on the opening of the channel crack is relaxed. Consequently, the steady-state energy release rate for the channel crack becomes greater than Eq. (1). A dimensional consideration leads to

$$G_{ss}^* = Z^* \left(\frac{d_s}{h_f}, \alpha, \beta \right) \frac{\sigma_f^2 h_f}{\bar{E}_f}, \quad (8)$$

where Z^* depends on the width of interfacial delamination (d_s/h_f) in addition to the elastic mismatch parameters. A finite element model [15] was employed to calculate G_{ss}^* , with the stable delamination width, d_s/h_f , obtained from Eq. (7) as a function of the normalized interface toughness, $\bar{\Gamma}_i$. As plotted in Fig. 4, the normalized driving force Z^* increases as $\bar{\Gamma}_i$ decreases and $Z^* \rightarrow \infty$ as $\bar{\Gamma}_i \rightarrow 0.5$, because interfacial delamination becomes unstable for $\bar{\Gamma}_i \leq 0.5$. Apparently, with interfacial delamination, the driving force for channel cracking can be significantly higher than that assuming no delamination, especially for the cases of compliant substrates ($\alpha > 0$).

While the interfacial delamination, if occurring, relaxes the constraint on crack opening thus enhances the fracture driving force, it also requires additional energy to fracture the interface as the channel crack advances. Considering the interfacial fracture energy, a modified fracture condition for steady-state growth of a channel crack can be written as

$$G_{ss}^* \geq \Gamma_f + W_d, \quad (9)$$

where Γ_f is the cohesive fracture toughness of the film, and W_d is the energy required to delaminate the interface accompanying per unit area growth of the channel crack. For stable delamination of width $d = d_s$ at both sides of a channel crack, the delamination energy is

$$W_d = \frac{2}{h_f} \int_0^{d_s} \Gamma_i(\psi(a)) da \approx \Gamma_i(\psi_{ss}) \frac{2d_s}{h_f}. \quad (10)$$

Equation (9) may not be convenient to apply directly, since both sides of the equation (driving force and resistance, respectively) increase with the interfacial delamination. By moving W_d to the left hand side and noting that the stable

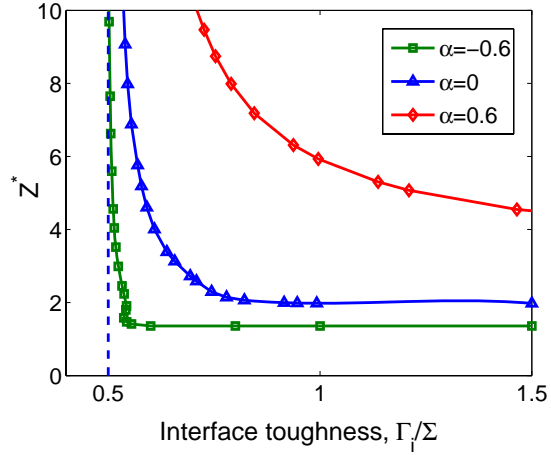


Fig. 4. Influence of the normalized interface toughness on the normalized energy release rate for steady-state channel cracking with interfacial delamination ($\Sigma = \sigma_f^2 h_f / \bar{E}_f$).

delamination width is a function of the interface toughness, we define an effective driving force for the steady-state channel cracking with delamination:

$$G_{eff}^* = G_{ss}^* - W_d = Z_{eff}^* (\bar{\Gamma}_i, \alpha, \beta) \frac{\sigma_f^2 h_f}{\bar{E}_f}, \quad (11)$$

with

$$Z_{eff}^* = Z^* \left(\frac{d_s}{h_f}, \alpha, \beta \right) - 2\bar{\Gamma}_i \frac{d_s}{h_f}. \quad (12)$$

Using the effective energy release rate, the condition for the steady-state channel cracking is simply a comparison between G_{eff}^* and Γ_f , the latter being a constant independent of the interface. Figure 5 plots the ratio, $Z_{eff}^*/Z(\alpha, \beta)$, as a function of $\bar{\Gamma}_i$ for different elastic mismatch parameters. At the limit of high interface toughness ($\bar{\Gamma}_i \rightarrow \infty$), $d_s \rightarrow 0$ and $Z_{eff}^* \rightarrow Z$, which recovers the case of channel cracking with no delamination. The effective driving force increases as the normalized interface toughness decreases.

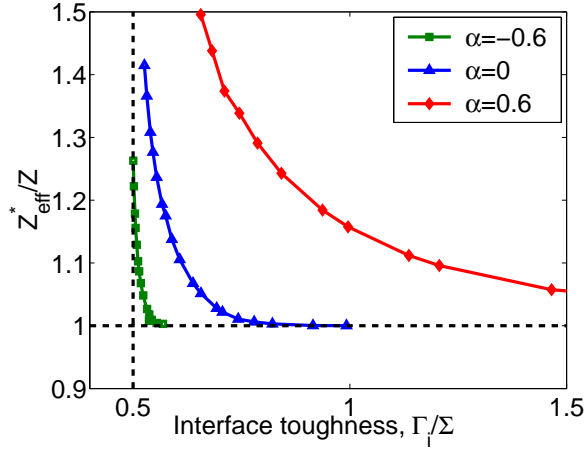


Fig. 5. Effective energy release rate for steady-state channel cracking as a function of the normalized interface toughness ($\Sigma = \sigma_f^2 h_f / \bar{E}_f$).

5. Channel Cracking with Substrate Penetration

In this section, crack penetrating into the substrate from the channel root (Fig. 1c) is analyzed. For an arbitrary penetration depth d_p , the energy release rate for substrate penetration is

$$G_p = Z_p \left(\frac{d_p}{h_f}, \alpha, \beta \right) \frac{\sigma_f^2 h_f}{\bar{E}_f}, \quad (13)$$

where Z_p is a dimensionless coefficient. A finite element model was employed to calculate Z_p as a function of the penetration depth for different elastic mismatch parameters, as plotted in Fig. 6. At the limit of short penetration cracks ($d_p/h_f \rightarrow 0$), the normalized energy release rate Z_p follows the same power law as Eq. (5) [14]. Therefore, the energy release rate for penetration approaches infinity for $\alpha > 0$ but remains bounded for $\alpha \leq 0$. Together with Fig. 2, it is predicted that for a stiff film on a compliant substrate ($\alpha > 0$), channel cracking of the film should inevitably be accompanied by either interfacial delamination or substrate penetration. The competition between delamination and penetration will

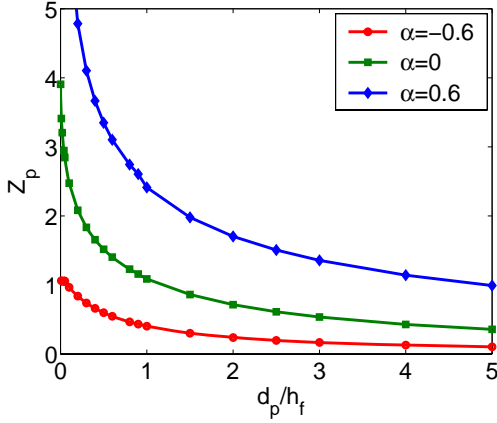


Fig. 6: Normalized energy release rate for substrate penetration as a function of the penetration depth.

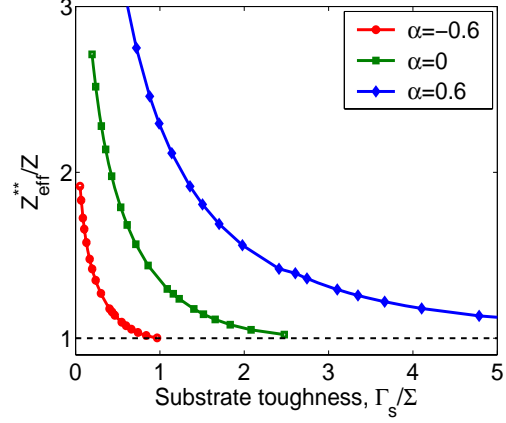


Fig. 7: Effective driving force for steady-state channel cracking with substrate penetration ($\Sigma = \sigma_f^2 h_f / \bar{E}_f$).

be further discussed in the next section. It can be seen that for $\alpha \geq 0$ the energy release rate for substrate penetration decreases monotonically with the depth and approaches zero as $d_p/h_f \rightarrow \infty$, suggesting stable growth of the penetration crack. The penetration depth can be obtained by setting

$$Z_p\left(\frac{d_p}{h_f}, \alpha, \beta\right) = \bar{\Gamma}_s = \frac{\bar{E}_f \Gamma_s}{\sigma_f^2 h_f}, \quad (14)$$

where Γ_s is fracture toughness of the substrate. It should be noted that the penetration crack growth may become unstable for substrates of finite thickness.

With a stable penetration crack into the substrate (Fig. 1c), the steady-state energy release rate for channel cracking becomes

$$G_{ss}^{**} = Z^{**}\left(\frac{d_p}{h_f}, \alpha, \beta\right) \frac{\sigma_f^2 h_f}{\bar{E}_f}, \quad (15)$$

where Z^{**} depends on the depth of the penetration and the elastic mismatch. Similar to the case of interfacial delamination, to account for the additional energy required to fracture the substrate, we define an effective driving force for the steady-state channel cracking with concomitant substrate penetration as

$$G_{eff}^{**} = Z_{eff}^{**}(\bar{\Gamma}_s, \alpha, \beta) \frac{\sigma_f^2 h_f}{\bar{E}_f}, \quad (16)$$

where

$$Z_{eff}^{**} = Z^{**}\left(\frac{d_p}{h_f}, \alpha, \beta\right) - \bar{\Gamma}_s \frac{d_p}{h_f} \quad (17)$$

As plotted in Fig. 7, the effective driving force increases as the normalized substrate toughness decreases.

6. Competition between Delamination and Penetration

As discussed above, both interfacial delamination and substrate penetration increase the driving force for channel cracking of brittle films, and both require additional energy to fracture either the interface or the substrate. By comparing the effective driving forces, the competition between delamination and penetration is discussed in this section.

First, for $\alpha = \beta = 0$, no interfacial delamination is predicted when $\bar{\Gamma}_i \geq 0.9878$, and no substrate penetration is possible when $\bar{\Gamma}_s \geq 3.952$. The two conditions correspond to two straight lines in Fig. 8a (normalized strain energy, Σ/Γ_s , versus the toughness ratio, Γ_i/Γ_s), dividing the plane into four regions: (I) no delamination and no penetration; (II) delamination only; (III) penetration only; (IV) both delamination and penetration are possible. In Region IV, interfacial delamination is favored when $Z_{eff}^* > Z_{eff}^{**}$ (Region IV-a) and substrate penetration is favored otherwise (IV-b). In Regions II and IV-a, the dashed line represents the condition $\bar{\Gamma}_i = 0.5$, beyond which interfacial delamination becomes unstable.

For a compliant substrate ($\alpha > 0$), both interfacial delamination and substrate penetration are possible over the entire plane as shown in Fig. 8b. By comparing the effective driving forces, interfacial delamination is favored when $Z_{eff}^* > Z_{eff}^{**}$ and substrate penetration is favored otherwise. It was found that stable interfacial delamination occurs only when $\Gamma_i/\Gamma_s < 0.5$.

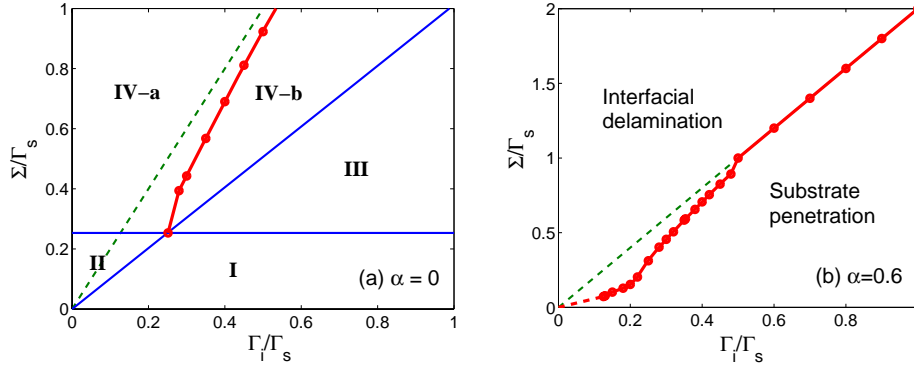


Fig. 8: Competition between interfacial delamination and substrate penetration at the root of a channel crack: (a) $\alpha = \beta = 0$, and (b) $\alpha = 0.6$.

7. Cohesive Zone Modeling of Delamination and Penetration

To further understand the competition between interfacial delamination and substrate penetration, we developed a cohesive zone model to simulate initiation and growth of delamination or penetration cracks from the root of a channel crack. A bilinear traction-separation law is used, with the elastic stiffness K , the

cohesive strength $\hat{\sigma}$, and the toughness Γ . For interfacial delamination, the effect of mode mix is accounted for by using a power-law fracture criterion

$$\frac{G_I}{\Gamma_I} + \frac{G_{II}}{\Gamma_{II}} = 1, \quad (18)$$

where G_I and G_{II} are the energy release rates for mode I and mode II, respectively, while Γ_I and Γ_{II} are the corresponding fracture toughness. For substrate penetration, only mode-I traction-separation law is needed. A finite element mesh near the root of a channel crack is shown in Fig. 9, with cohesive elements along the interface and straight ahead in the substrate.

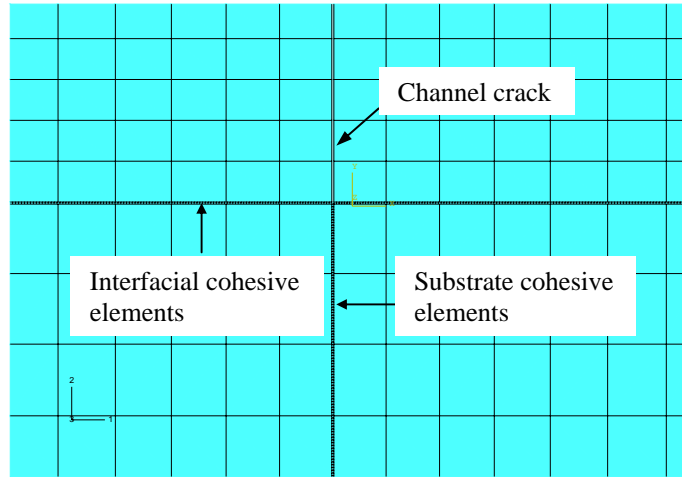


Fig. 9: Finite element mesh for simulating competition between interfacial delamination and substrate penetration from the root of a channel crack.

Two examples are shown in Fig. 10, one with interfacial delamination and the other with substrate penetration. Here the elastic properties of the film and substrate materials are identical, and the same traction-separation law is used for the substrate. In Fig. 10(a), the interface has a lower toughness, while in Fig. 10(b) the interface toughness is higher than the substrate. A systematic comparison between numerical simulations by the cohesive zone model and the predictions by the linear elastic fracture mechanics is currently in progress.

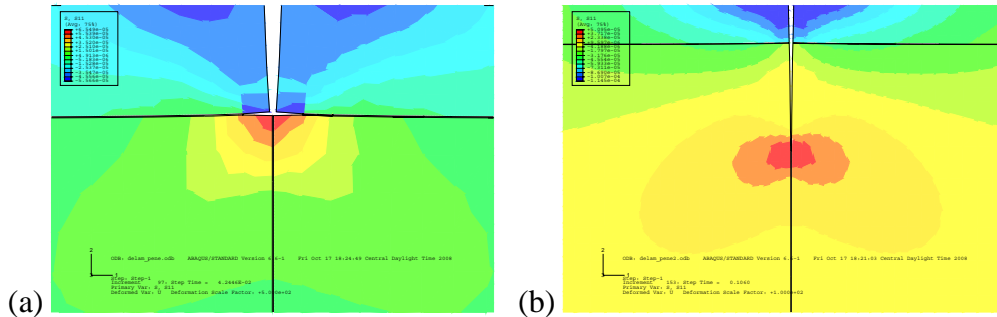


Fig. 10. Numerical simulations by the cohesive zone model, showing (a) interfacial delamination and (b) substrate penetration from the root of a channel crack.

References

- [1] P.S. Ho, G. Wang, M. Ding, J.H. Zhao, X. Dai, Reliability issues for flip-chip packages, *Microelectronics Reliability* 44 (2004) 719-737.
- [2] X.H. Liu, M.W. Lane, T.M. Shaw, E.G. Liniger, R.R. Rosenberg, D.C. Edelstein, Low-k BEOL mechanical modeling, *Proc. Advanced Metallization Conference* (2004) 361-367.
- [3] T.Y. Tsui, A.J. McKerrow, J.J. Vlassak, Constraint effects on thin film channel cracking behavior, *J. Mater. Res.* 20 (2005) 2266-2273.
- [4] S. Wagner, S.P. Lacour, J. Jones, P.I. Hsu, J.C. Sturm, T. Li, Z. Suo, Electronic skin: architecture and components, *Physica E* 25 (2004) 326-334.
- [5] D.Y. Khang, H.Q. Jiang, Y. Huang, J.A. Rogers, A stretchable form of single-crystal silicon for high-performance electronics on rubber substrate, *Science* 311 (2006) 208-212.
- [6] J.W. Hutchinson, Z. Suo, Mixed mode cracking in layered materials, *Advances in Applied Mechanics* 29 (1992) 63-191.
- [7] J.L. Beuth, Cracking of thin bonded film in residual tension, *Int. J. Solids Struct.* 29 (1992) 1657-1675.
- [8] R. Huang, J.H. Prevost, Z.Y. Huang, Z. Suo, Channel-cracking of thin films with the extended finite element method, *Eng. Frac. Mech.* 70 (2003) 2513-2526.
- [9] J.M. Ambrico, M.R. Begley, The role of initial flaw size, elastic compliance and plasticity in channel cracking of thin films, *Thin Solid Films* 419 (2002) 144-153.
- [10] R. Huang, J.H. Prevost, Z. Suo, Loss of constraint on fracture in thin film structures due to creep, *Acta Mater.* 50 (2002) 4137-4148.
- [11] Z. Suo, J.H. Prevost, J. Liang, Kinetics of crack initiation and growth in organic-containing integrated structures, *J. Mech. Phys. Solids* 51 (2003) 2169-2190.
- [12] N. Cordero, J. Yoon, Z. Suo, Channel cracks in hermetic coating consisting of organic and inorganic layers, *Appl. Phys. Lett.* 90 (2007) 111910.
- [13] M.Y. He, J.W. Hutchinson, Crack deflection at an interface between dissimilar elastic materials, *Int. J. Solids Struct.* 25 (1989) 1053-1067.
- [14] T. Ye, Z. Suo, A.G. Evans, Thin film cracking and the roles of substrate and interface, *Int. J. Solids Struct.* 29 (1992) 2639-2648.
- [15] H. Mei, Y. Pang, R. Huang, Influence of interfacial delamination on channel cracking of elastic thin films, *Int. J. Fracture* 148 (2007) 331-342.
- [16] J.P. Parmigiani, M.D. Thouless, The roles of toughness and cohesive strength on crack deflection at interfaces, *J. Mech. Phys. Solids* 54 (2006), 266-287.
- [17] K. Hayashi, S. Nemat-Nasser, Energy-release rate and crack kinking under combined loading, *J. Appl. Mech.* 48 (1981) 520-524.
- [18] Z. Suo, J.W. Hutchinson, Interface crack between two elastic layers. *Int. J. Fracture* 43 (1990) 1-18.